

# Coadsorption of Nitrogen Dioxide and Oxygen on Pt(111)<sup>†</sup>

M. E. Bartram, R. G. Windham, and B. E. Koel\*

Cooperative Institute for Research in Environmental Sciences (CIRES) and the Department of Chemistry and Biochemistry, University of Colorado at Boulder, Boulder, Colorado 80309-0449

Received July 16, 1987. In Final Form: October 30, 1987

Temperature-programmed desorption (TPD) and high-resolution electron energy loss spectroscopy (HREELS) have been used to determine the NO<sub>2</sub> adsorption energy and geometry in the presence of coadsorbed oxygen atoms on Pt(111) at 100 K. NO<sub>2</sub> is adsorbed molecularly, regardless of the oxygen atom precoverage. Coadsorption with oxygen atoms causes a decrease in the amount of irreversible NO<sub>2</sub> adsorption and also a decrease in the amount of the Pt(111)  $\mu$ -N,O-nitrito surface complex (bridge-bonded NO<sub>2</sub>). Coadsorption also causes the formation of a new, low-temperature desorption state for NO<sub>2</sub> which is associated with an NO<sub>2</sub> bonding geometry possessing C<sub>2v</sub> symmetry. It is proposed that this NO<sub>2</sub> species is bonded to a platinum atom through the nitrogen atom in a nitro configuration. An NO<sub>3</sub> species is not observed spectroscopically at any oxygen atom coverage in this work. However, an NO<sub>3</sub> intermediate may be responsible for some of the features in the adsorption and desorption kinetics. At  $\theta_O = 0.75$  monolayer (ML), a chemisorbed NO<sub>2</sub> saturation coverage of 0.15 ML can be achieved and all NO<sub>2</sub> adsorption is reversible, having a chemisorption bond energy of 11 kcal/mol. When the chemisorbed state is saturated, an N<sub>2</sub>O<sub>4</sub> multilayer can be formed at 100 K with greater NO<sub>2</sub> exposures.

## Introduction

It has recently been established by using temperature-programmed desorption (TPD) and high-resolution electron energy loss spectroscopy (HREELS) that NO<sub>2</sub> is adsorbed molecularly at all coverages on clean Pt(111) at 100 K.<sup>1</sup> NO<sub>2</sub> is bonded to this surface exclusively with C<sub>s</sub> symmetry as a Pt(111)  $\mu$ -N,O-nitrito surface complex bridge-bonded between two platinum atoms via an oxygen atom and the nitrogen atom. This surface species is thought to be the necessary precursor to the dissociation of NO<sub>2</sub> that produces adsorbed oxygen atoms and NO when the surface temperature is raised to 170 K. When  $\theta_{NO_2} = 0.25$  monolayer (ML), the resulting combined oxygen atom and NO coverage is 0.5 ML and the surface becomes passivated to a degree. NO<sub>2</sub> desorption from greater coverages then becomes competitive with its dissociation.

Schwalke et al.<sup>2</sup> have observed that after initial NO<sub>2</sub> decomposition on Ru(001) at 80 K the surface becomes passivated with the decomposition products oxygen atoms and NO. Further NO<sub>2</sub> adsorption is molecular. NO<sub>2</sub> is bonded to the surface with C<sub>2v</sub> symmetry via the nitrogen atom in a nitro-bonded configuration. This implies that the nitro adsorption geometry is not the required precursor for dissociation and that Ru(001) is too reactive for the adsorbed NO<sub>2</sub> configuration required for dissociation to be observed spectroscopically.

The NO<sub>2</sub>/Ru(001) system is an interesting contrast to the NO<sub>2</sub>/Pt(111) system. As long as bridge-bonded NO<sub>2</sub> is available on Pt(111), decomposition continues to take place when the temperature is raised to 170 K. If the possibility for adsorption in a bridge-bonded geometry is removed, the decomposition pathway for NO<sub>2</sub> should be eliminated on Pt(111).

This paper reports the use of coadsorbed oxygen atom coverages as high as 0.75 ML on Pt(111) to investigate modifications in the NO<sub>2</sub> adsorption energy and geometry. At coverages of  $\theta_O \geq 0.25$  ML, in addition to bridge-bonded NO<sub>2</sub>, NO<sub>2</sub> is found to bond to the surface in the same nitro-bonded configuration that has been observed for NO<sub>2</sub> molecularly adsorbed on Ru(001). When  $\theta_O = 0.75$  ML, NO<sub>2</sub> can only bond to Pt(111) in a nitro-bonded geometry

and NO<sub>2</sub> decomposition no longer takes place upon warming the sample. Schematic potential energy diagrams are used to rationalize this behavior qualitatively. In addition, we have studied the subtle changes that take place in the low-temperature physisorption states when the Pt(111) surface is precovered with oxygen atoms. This report is one in an on-going series that examines the adsorption and bonding of nitrogen oxides on metal surfaces.<sup>1,3</sup>

## Experimental Section

The experiments were carried out in a stainless steel UHV system that has been described previously.<sup>1,4</sup> The system contains the instrumentation necessary to perform HREELS, TPD, Auger electron spectroscopy (AES), and low-energy electron diffraction (LEED). The crystal is heated resistively and is cooled by direct contact between the crystal holder and a liquid nitrogen reservoir. The temperature of the crystal is monitored by a chromel-alumel thermocouple. All data acquisition is accomplished under computer control except for the LEED observations.

Details concerning the Pt(111) crystal used in these experiments and the manner in which it was cleaned and characterized are available elsewhere.<sup>1</sup> The procedure used to synthesize and store the high-purity NO<sub>2</sub>, the description of the microcapillary array doser used for NO<sub>2</sub> exposures and the flux enhancement factor achieved with it, the method used to calibrate the coverages of reversibly and irreversibly adsorbed NO<sub>2</sub>, and the method used for the TPD and HREELS experiments have been given previously.<sup>1</sup> The only exception is that a 8 K/s heating ramp was used for TPD in these experiments.

All of the HREELS spectra, including those of the warm-up experiments, were taken with the crystal at 100 K. Signal-averaging with repetitive scans in combination with a real-time display of energy losses allowed features due to impurities adsorbed from the background such as NO to be easily identified.

The oxygen atom coverages used in this work were generated by exposing the crystal to NO<sub>2</sub> at 400 K.<sup>5,6</sup> The coverages were measured with AES using the calibration established in ref 5. Oxygen atom and NO<sub>2</sub> coverages reported in this paper are referenced to the Pt(111) substrate.

(1) Bartram, M. E.; Windham, R. G.; Koel, B. E. *Surf. Sci.* 1987, 184, 57.

(2) Schwalke, U.; Parmeter, J. E.; Weinberg, W. H. *J. Chem. Phys.* 1986, 84, 4036.

(3) Bartram, M. E.; Koel, B. E. *Surf. Sci.*, submitted.

(4) Windham, R. G.; Bartram, M. E.; Koel, B. E. *J. Phys. Chem.*, submitted.

(5) Parker, D. H.; Bartram, M. E.; Koel, B. E. *Surf. Sci.*, submitted.

(6) Segner, J.; Vielhaber, W.; Ertl, G. *Isr. J. Chem.* 1982, 22, 375.

<sup>†</sup> Presented at the symposium entitled "Molecular Processes at Solid Surfaces: Spectroscopy of Intermediates and Adsorbate Interactions", 193rd National Meeting of the American Chemical Society, Denver, CO, April 6-8, 1987.

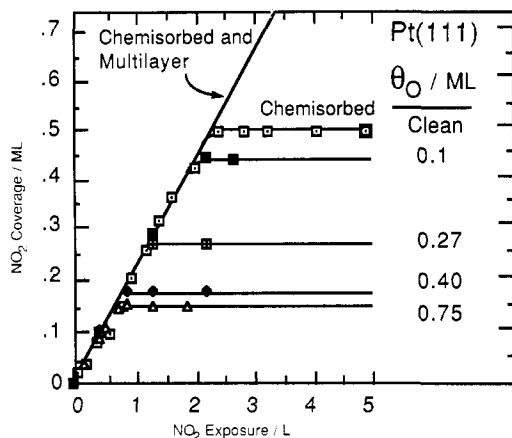


**Figure 1.**  $\text{NO}_2$  uptake curves for several oxygen atom precoverages on Pt(111) at 100 K. The curves are derived from integrated thermal desorption data. A dramatic precursor effect dominates the  $\text{NO}_2$  uptake in all cases, and the  $\text{NO}_2$  initial sticking coefficient is independent of the surface oxygen coverage.

### Results

**Temperature-Programmed Desorption and  $\text{NO}_2$  Uptake.** TPD experiments were performed as a function of  $\text{NO}_2$  exposure at 100 K with several precoverages of oxygen atoms on Pt(111). Chemisorbed  $\text{NO}_2$  was formed from low exposures of  $\text{NO}_2$ . The desorption of  $\text{NO}_2$  from this state followed first-order kinetics and was detected by monitoring mass 46. This provided a measure of reversibly adsorbed  $\text{NO}_2$ . Irreversibly adsorbed  $\text{NO}_2$  decomposed to NO and oxygen atoms. Monitoring mass 30 for NO during TPD provided a measure of  $\text{NO}_2$  irreversible adsorption. The desorption of  $\text{O}_2$  from oxygen atom recombination on the surface took place at temperatures well above the desorption states for NO and  $\text{NO}_2$ .  $\text{O}_2$  desorption was detected by monitoring mass 32. The oxygen atoms resulting from irreversible  $\text{NO}_2$  adsorption did not create any new features in the  $\text{O}_2$  desorption spectra that have been reported for high oxygen atom coverages on Pt(111).<sup>5</sup> Physisorbed  $\text{N}_2\text{O}_4$  multilayers were formed from higher exposures of  $\text{NO}_2$ .<sup>1</sup> But only mass 46 was observed during desorption from the multilayer. Desorption from the chemisorbed  $\text{NO}_2$  and physisorbed  $\text{N}_2\text{O}_4$  states can be distinguished, however, by the lower desorption temperature of  $\text{NO}_2$  from the physisorbed state. Physisorbed states of  $\text{N}_2\text{O}_4$  are removed by heating to 170 K. The assignments of the  $\text{NO}_2$  and  $\text{N}_2\text{O}_4$  species in the two states are supported by HREELS results, which will be discussed in the next subsection.

The results of each set of TPD experiments are summarized by using the integrated thermal desorption data to construct the uptake curves shown in Figure 1. Each curve that ends as a horizontal line in Figure 1 represents the sum of reversibly and irreversibly chemisorbed  $\text{NO}_2$  for a given oxygen atom precoverage. The straight line that is common to each of the uptake curves and which extends above the uptake curve for chemisorption on the clean surface represents the amount of  $\text{NO}_2$  adsorbed in both the chemisorbed and physisorbed states as a function of exposure. The data points used to construct the upper portion of this line have been left out of the figure for clarity. The fact that this line is common to each uptake curve indicates that the sticking coefficient for  $\text{NO}_2$  is the same for chemisorption as it is for physisorption. It also indicates that the  $\text{NO}_2$  initial sticking coefficient is constant and independent of the preadsorbed oxygen atom coverage. The initial slope of each curve matches the slope of the curve for the clean Pt(111) surface, determined previously to represent a sticking coefficient of unity.<sup>1</sup> The high sticking coefficient and the shape of the uptake curve

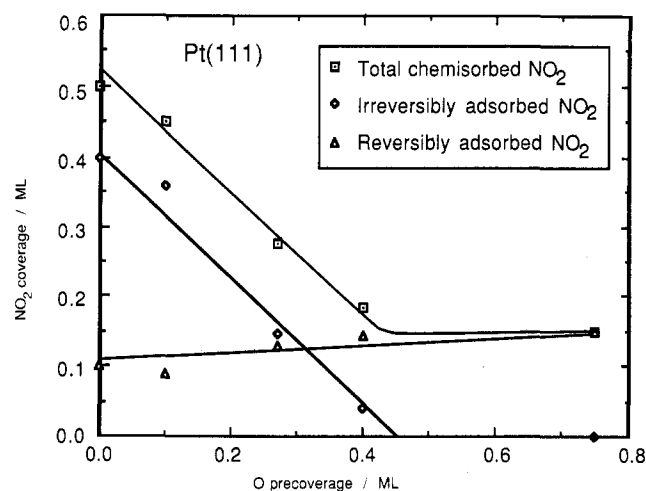


**Figure 2.** Saturation coverages of chemisorbed  $\text{NO}_2$  as a function of oxygen atom precoverage on Pt(111). The amount of irreversibly adsorbed  $\text{NO}_2$  decreases to zero when the precoverage of oxygen atoms reaches 0.45 ML.

have been attributed for Pt(111) to the existence of precursor states that can be populated with a high probability due to the availability of a large number of short-lived adsorption intermediates for  $\text{NO}_2$ .<sup>1</sup> Considering that oxygen atoms are present on the surface, an important factor in the adsorption kinetics may be the formation of an  $\text{NO}_3$  intermediate. This subject will be treated in greater detail in the Discussion section.

For the  $\text{NO}_2$  uptake curve at  $\theta_{\text{O}} = 0.75$  ML, the initial slope and the saturation chemisorption coverage are both the same whether adsorption takes place at 100 or 170 K. Exposures at 170 K were performed to remove the possibility of any features of physisorbed layers being included in the integration. Besides having the same initial sticking coefficients of unity, the  $\theta_{\text{O}} = 0.75$  ML and the clean uptake curves also have similar functional forms versus exposure with relatively abrupt breakpoints. This allowed the other curves in Figure 1 to be adequately characterized by determining the onset of the multilayer formation for each oxygen coverage.

It is clear from Figure 1 that the saturation coverage of chemisorbed  $\text{NO}_2$  decreases as the oxygen atom precoverage increases. The specific dependence is shown in Figure 2 to be the result of two effects by plotting the amount of  $\text{NO}_2$  that is irreversibly and reversibly adsorbed, in addition to the total chemisorbed coverage, as a function of oxygen atom precoverage. Up to precoverages of  $\theta_{\text{O}} = 0.45$  ML,  $\text{NO}_2$  uptake and the amount of irreversibly adsorbed  $\text{NO}_2$  are reduced linearly. We attribute this to simple site-blocking by oxygen atoms on the surface. The slope of these lines implies that one adsorbed  $\text{NO}_2$  is eliminated for every preadsorbed oxygen atom. This is in contrast to the amount of  $\text{NO}_2$  that is reversibly adsorbed. At least 0.1 ML of  $\text{NO}_2$  is reversibly adsorbed for each saturation  $\text{NO}_2$  coverage, reaching a maximum of 0.15 ML on the oxygen-saturated surface. Thus, this state is largely independent of oxygen atom precoverage. The HREELS spectra will be used in the next subsection to show that nitro-bonded  $\text{NO}_2$  populates this state at  $\theta_{\text{O}} = 0.25$  ML and above. Thus, nitro-bonded  $\text{NO}_2$  becomes an adsorption alternative that allows the surface to be populated by  $\text{NO}_2$  at oxygen atom coverages where the uptake of bridge-bonded  $\text{NO}_2$  would otherwise be expected to go to zero. If the coadsorbed oxygen atoms that result from  $\text{NO}_2$  decomposition during TPD are considered, then the total oxygen atom coverage including preadsorbed oxygen atoms is essentially constant up to an oxygen precoverage of 0.45 ML. Above this value, where essentially no  $\text{NO}_2$  decom-

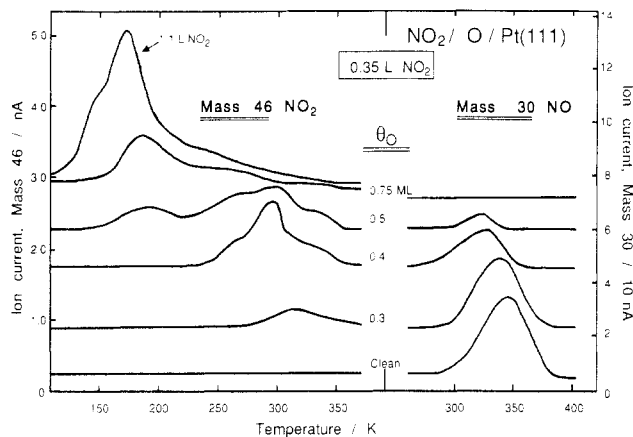


**Figure 3.**  $\text{NO}_2$  and  $\text{NO}$  desorption spectra resulting from oxygen atom precovered  $\text{Pt}(111)$  exposed to 0.35 langmuir of  $\text{NO}_2$  at 100 K. This exposure provides the same initial coverage of  $\text{NO}_2$  for each experiment.

position takes place, the oxygen atom coverage is due only to the oxygen atoms that are preadsorbed.

It can be seen from Figure 1 that exposures below 0.75 langmuir provide the same amount of chemisorbed  $\text{NO}_2$  regardless of the amount of preadsorbed oxygen that is on the surface. Using a constant exposure of 0.35 langmuir for a series of TPD experiments as a function of oxygen atom precoverage provides a point that is common to each uptake curve. These desorption spectra show in Figure 3 the manner in which the energetics of the desorption states for  $\text{NO}_2$  change as a function of oxygen atom precoverage. No desorption of  $\text{NO}_2$  is seen on the clean  $\text{Pt}(111)$  surface from an  $\text{NO}_2$  exposure of 0.35 langmuir.<sup>1</sup> When  $\theta_{\text{O}} = 0.3$  ML, some reversible adsorption of  $\text{NO}_2$  is observed at 310 K. This corresponds to an activation energy for desorption of 19 kcal/mol and is similar to that observed for  $\text{NO}_2$  exposures of 1.5 langmuir and greater on clean  $\text{Pt}(111)$ . At 0.4 ML of oxygen atoms, a greater amount of  $\text{NO}_2$  is reversibly adsorbed with a decrease in the activation energy for desorption. By 0.5 ML of oxygen atoms however, the amount of  $\text{NO}_2$  that desorbs from this state is diminished, and desorption from a new state is seen at 180 K. When the surface is saturated with oxygen atoms at  $\theta_{\text{O}} = 0.75$  ML, the high-temperature desorption state of  $\text{NO}_2$  is absent and the low-temperature desorption state is populated to a greater extent. It is saturated by 1.1 langmuir of  $\text{NO}_2$ . Desorption from this state takes place with first-order kinetics and  $E_a = 11$  kcal/mol. The high-temperature tail for this desorption may be the result of the low degree of order of the oxygen-saturated  $\text{Pt}(111)$  surface and/or some interconversion of the two  $\text{NO}_2$  states.

Directly associated with these changes in the desorption kinetics for molecular  $\text{NO}_2$  is the reduction in the amount of  $\text{NO}_2$  that is dissociated to oxygen atoms and  $\text{NO}$  upon warming. This can be seen in Figure 3 from the decrease in the amount of  $\text{NO}$  that desorbs as the oxygen atom precoverage increases. When  $\theta_{\text{O}} = 0.75$  ML, no  $\text{NO}$  desorbs, signifying that all  $\text{NO}_2$  adsorption is reversible. The energy of activation for the first-order desorption of  $\text{NO}$  shown in Figure 3 decreases continuously with increasing oxygen atom coverage in a similar way to that seen previously for  $\text{NO}$  desorbing from  $\text{Pt}(111)$  when coadsorbed with other electronegative coadsorbates.<sup>1,7,8</sup>

When the surface saturated with oxygen atoms is given further exposures to  $\text{NO}_2$ , two more low-temperature  $\text{NO}_2$  desorption states are populated. HREELS spectra show that these states are populated by an  $\text{N}_2\text{O}_4$  physisorbed species. The vibrational spectra are discussed in the next

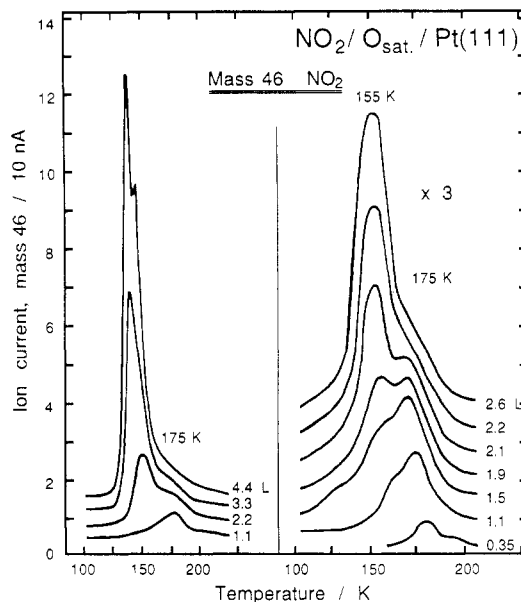


**Figure 4.**  $\text{NO}_2$  desorption spectra from oxygen atom saturated  $\text{Pt}(111)$  for several  $\text{NO}_2$  exposures at 100 K. By 3.3 langmuirs, the zero-order desorption of  $\text{NO}_2$  from an  $\text{N}_2\text{O}_4$  multilayer begins with an onset at 120 K. Exposures less than this are associated with first-order desorption from a physisorbed state with a peak maximum at 155 K that is distinctly different from the chemisorbed state at 175 K.

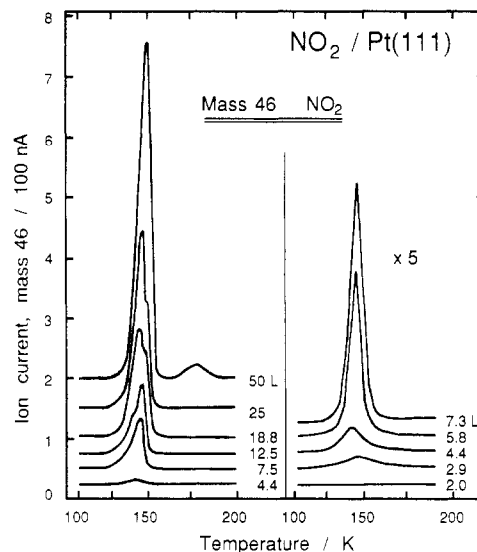


**Figure 5.**  $\text{NO}_2$  desorption spectra from several  $\text{N}_2\text{O}_4$  multilayer coverages on bridge-bonded  $\text{NO}_2$ -saturated  $\text{Pt}(111)$ . Saturation of a zero-order desorption state at 12.5 langmuirs is followed by desorption from a different zero-order desorption state.

subsection. The first state is populated by  $\text{NO}_2$  exposures greater than 1.1 langmuirs. The desorption of  $\text{NO}_2$  from this state at 155 K follows first-order kinetics and is shown in detail on the right-hand side of Figure 4. The left-hand side of Figure 4 shows that this state is saturated by approximately 3.3 langmuirs of  $\text{NO}_2$ . At this exposure a second  $\text{NO}_2$  desorption state begins to form. The desorption takes place with zero-order kinetics with an onset of 120 K. The double peak seen in the desorption spectrum that corresponds to the 4.4-langmuir exposure is reproducible and suggests the possibility that the two physisorption states may become populated competitively at this coverage. Considering that the chemisorbed state is saturated by 1.1 langmuirs and that the multilayer begins at an exposure of approximately 3.3 langmuirs, the  $\text{NO}_2$  exposure difference of 2.2 langmuirs is required to saturate the 155 K first-order desorption state. Since the  $\text{NO}_2$  sticking coefficient is unity, this exposure indicates

(7) Gorte, R. J.; Schmidt, L. D.; *Surf. Sci.* **1981**, *111*, 260.

(8) Bartram, M. E.; Windham, R. G.; Koel, B. E. *Surf. Sci.*, submitted.

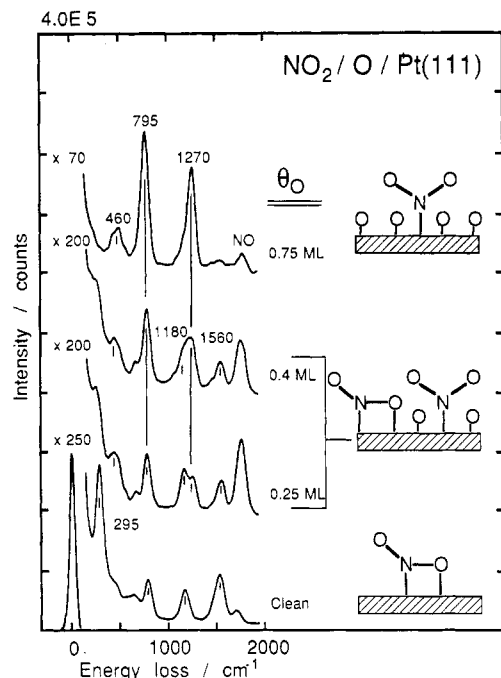


**Figure 6.** HREELS spectra for NO<sub>2</sub> adsorbed at 170 K with increasing amounts of oxygen atoms on Pt(111).

that an N<sub>2</sub>O<sub>4</sub> coverage on the order of 0.25 ML is associated with this desorption state.

The desorption spectra of NO<sub>2</sub> from N<sub>2</sub>O<sub>4</sub> on oxygen atom saturated Pt(111) are uniquely different from the desorption spectra of NO<sub>2</sub> from N<sub>2</sub>O<sub>4</sub> observed on the bridge-bonded NO<sub>2</sub>-saturated Pt(111) surface (in the absence of coadsorbed oxygen atoms) that are shown in Figure 5. This difference may be due to the existence of metastable NO<sub>3</sub>. In Figure 5, two physisorbed NO<sub>2</sub> desorption states other than the NO<sub>2</sub> chemisorbed state can also be populated. However, neither of these desorbs with first-order kinetics. The right-hand side of Figure 5 shows that the first of these states begins to be populated by 2.6 langmuirs of NO<sub>2</sub> with an onset of 125 K. The overlap of the leading edges of the desorption curves from greater coverages of NO<sub>2</sub> make it clear that desorption of NO<sub>2</sub> from this state is governed by zero-order kinetics. As shown on the left side of Figure 5, saturation is reached at about 12.5 langmuirs. The NO<sub>2</sub> exposure difference of 9.6 langmuirs that is necessary for saturation implies that approximately 1 ML of N<sub>2</sub>O<sub>4</sub> populates this state. At this point the zero-order desorption of NO<sub>2</sub> from a second state begins at an onset of 120 K. This multilayer of N<sub>2</sub>O<sub>4</sub> can be populated without limit with greater exposures of NO<sub>2</sub>. The desorption of NO<sub>2</sub> at 180 K has been noted previously,<sup>1</sup> but the origin of this state is not understood.

**High-Resolution Electron Energy Loss Spectroscopy.** The dependence of the chemisorbed NO<sub>2</sub> bonding geometry on oxygen atom coverage was explored in a series of HREELS experiments. The population of physisorption states was avoided by carrying out the NO<sub>2</sub> exposures at 170 K. The spectra are shown in Figure 6. Energy losses at 460 cm<sup>-1</sup> are due to the Pt-O stretch for preadsorbed oxygen atoms.<sup>5,9</sup>

On the clean Pt(111) surface in Figure 6, losses are seen that are due to a Pt(111)  $\mu$ -N,O-nitrito surface complex possessing C<sub>s</sub> symmetry (bridge-bonded NO<sub>2</sub>) that has been reported previously.<sup>1</sup> The ONO asymmetric stretch occurs at 1560 cm<sup>-1</sup>, the ONO symmetric stretch at 1180 cm<sup>-1</sup>, the ONO bend at 795 cm<sup>-1</sup>, and the Pt-molecule stretch at 295 cm<sup>-1</sup>. The high-frequency loss at 1740 cm<sup>-1</sup>

**Table I. Vibrational Frequencies (cm<sup>-1</sup>) of Nitro-Bonded NO<sub>2</sub> on O-Saturated Pt(111) Compared to Gas-Phase NO<sub>2</sub>,<sup>16</sup> the Free Nitrite Ion Found in NaNO<sub>2</sub>,<sup>10</sup> and Nitro-Bonded NO<sub>2</sub> in a Pt Coordination Compound<sup>10</sup>**

mode	NO <sub>2</sub> /O/ Pt(111) <sup>a</sup>	NO <sub>2</sub> (g)	NO <sub>2</sub> <sup>-</sup>	Pt(NO <sub>2</sub> ) <sub>4</sub> <sup>2-</sup>	NO <sub>2</sub> / Ru(001) <sup>b</sup>
$\delta$ NO <sub>2</sub> (bend)	795	750	830	838-845	780
$\nu_s$ ONO (sym stretch)	1270	1318	1335	1344-1392	1300
$\nu_a$ ONO (asym stretch)		1618	1250	1415-1440	

<sup>a</sup> This work. <sup>b</sup> NO<sub>2</sub> coadsorbed with NO and O on Ru(001).<sup>2</sup>

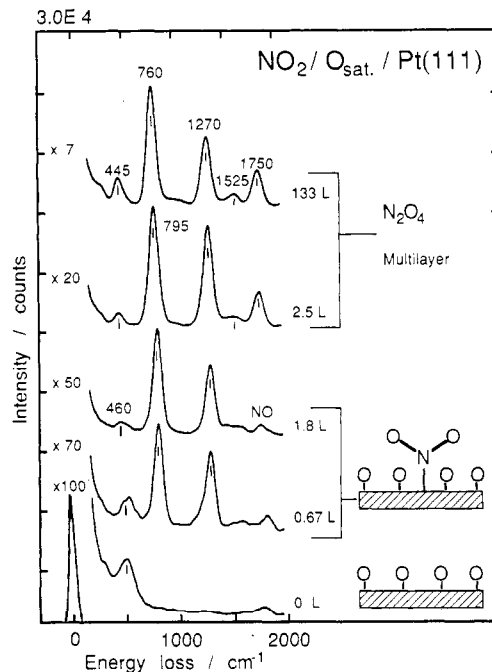


**Figure 7.** HREELS spectra for increasing NO<sub>2</sub> exposures to oxygen atom saturated Pt(111) at 100 K.

is due to the stretch of a top-site bonded coadsorbed NO impurity. The loss due to this impurity is present in each of the spectra and shifts to a higher frequency with increasing amounts of coadsorbed oxygen atoms.<sup>8</sup> The frequency of the Pt-NO stretch when NO is coadsorbed with oxygen atoms is at 265 cm<sup>-1</sup>.

When NO<sub>2</sub> is adsorbed with an increasing amount of oxygen atoms on Pt(111), a loss due to a new species grows in at 1270 cm<sup>-1</sup> while the losses due to bridge-bonded NO<sub>2</sub> become less intense. At intermediate oxygen atom coverages, therefore, two NO<sub>2</sub> adsorption isomers are present at the same time. On the surface saturated with oxygen atoms at  $\theta_0 = 0.75$  ML, energy losses having the frequencies associated with the ONO asymmetric and symmetric stretches of bridge-bonded NO<sub>2</sub> are present with only minimal intensity. The HREELS spectrum of this surface indicates that NO<sub>2</sub> is adsorbed in a geometry that is distinctly different from that found on the clean Pt(111) surface. This is consistent with the TPD results which show that NO<sub>2</sub> is only reversibly adsorbed on the oxygen-saturated surface. The energy loss at 1270 cm<sup>-1</sup> is in the frequency range seen for the ONO symmetric stretch in a number of transition-metal NO<sub>2</sub> coordination compounds<sup>10</sup> and is of a similar frequency at the same mode for NO<sub>2</sub> adsorbed in a nitro configuration with C<sub>2v</sub> symmetry on Ru(001).<sup>2</sup> These vibrational frequencies are given in Table I for comparison.

All of the peaks were attenuated in off-specular scans, and no other modes were observed. Therefore, all of the

(9) Gland, J. L.; Sexton, B. A.; Fisher, G. B. *Surf. Sci.* 1980, 95, 587.

(10) Hitchman, M. A.; Rowbottom, G. L. *Coord. Chem. Rev.* 1982, 42, 55.

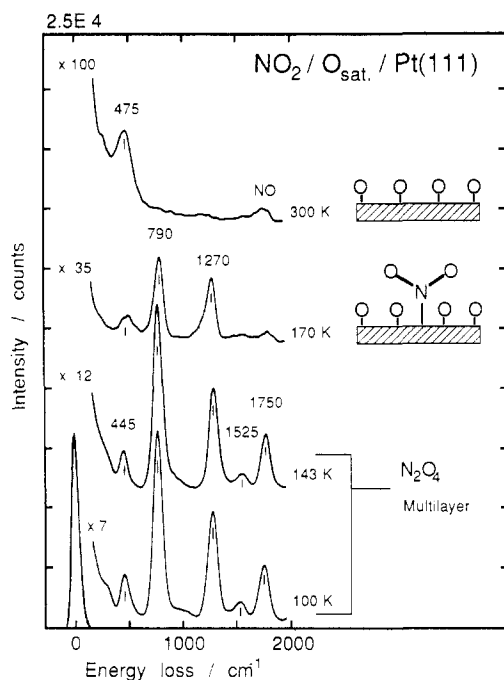
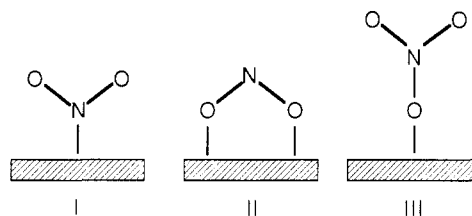


**Figure 8.** HREELS warm-up experiments for the oxygen atom saturated Pt(111) surface after a 133-langmuir  $\text{NO}_2$  exposure at 100 K.

observed losses in Figure 6 are due to dipole scattering. In accordance with the surface dipole-selection rule,<sup>11,12</sup> the disappearance of the asymmetric ONO stretching mode is associated with the adsorption of  $\text{NO}_2$  in a geometry of higher symmetry than  $C_s$ .  $\text{NO}_2$  bonded to the surface with  $C_{2v}$  symmetry would be consistent with this and would allow only the ONO bend and symmetric stretch to be observed with on-specular HREELS. Interestingly, the frequency of the  $\text{NO}_2$  bending mode is typically insensitive to the  $\text{NO}_2$  bonding geometry.<sup>10</sup> A constant value of 795  $\text{cm}^{-1}$  seen in Figure 6 is in close agreement with the bending mode of  $\text{NO}_2$  found on other surfaces.<sup>1-3,13</sup>

The vibrational spectra in Figure 6 combined with the desorption spectra in Figure 3 at similar oxygen atom precoverages show that decomposition of  $\text{NO}_2$  to NO and oxygen atoms only occurs when  $\text{NO}_2$  is adsorbed in a bridge-bonded geometry. On the oxygen atom saturated surface, where  $\text{NO}_2$  is bonded to the surface exclusively in a nitro configuration,  $\text{NO}_2$  decomposition does not occur. This further confirms that bridge-bonded  $\text{NO}_2$  is the required precursor to  $\text{NO}_2$  dissociation.

Figure 7 shows the results of a set of HREELS experiments that were performed as a function of  $\text{NO}_2$  exposure on oxygen atom saturated ( $\theta_0 = 0.75$  ML) Pt(111) at 100 K. Initially, only the Pt-O stretch at 460  $\text{cm}^{-1}$  is observed. As in Figure 6, 0.67 langmuir of  $\text{NO}_2$  at 100 K on the oxygen-saturated surface gives energy losses that can be assigned to  $C_{2v}$   $\text{NO}_2$ . At 1.8 langmuirs, an exposure that is sufficient to saturate the chemisorbed state, no changes take place in the spectra except an increase in the intensities of the losses. An exposure of 2.5 langmuirs provides a coverage that corresponds to the first-order desorption state seen at 155 K. The HREELS spectrum has intense losses at frequencies like that seen for  $\text{N}_2\text{O}_4$  on other surfaces.<sup>1-3</sup> The  $\text{N}_2\text{O}_4$  losses become much more intense at an  $\text{NO}_2$  exposure large enough to populate the zero-order desorption state.



When the  $\text{N}_2\text{O}_4$  multilayer is warmed up, as shown in Figure 8, there is a decrease in the intensities at 143 K. Other than this, however, there are no changes in the spectra until 170 K. At this temperature, all features of the multilayer are gone, leaving only those of  $\text{NO}_2$  chemisorbed with  $C_{2v}$  symmetry. There is no detectable conversion to bridge-bonded  $\text{NO}_2$  that takes place during the warmup nor does any  $\text{NO}_2$  decompose. Consistent with the TPD results, the spectra in Figure 8 show that all of the  $\text{NO}_2$  has desorbed from the surface by 300 K.

**LEED.** LEED observations of adsorbed  $\text{NO}_2$  were made under a number of conditions. These used different oxygen atom precoverages for a basis set of experiments in which the exposures of  $\text{NO}_2$  were varied and also a thick  $\text{N}_2\text{O}_4$  multilayer was warmed up. No difference in the surface order of the oxygen atom covered surfaces<sup>5</sup> was detected upon  $\text{NO}_2$  coadsorption under any of the conditions studied.

## Discussion

**Bonding Geometry of  $\text{NO}_2$ .** Although  $\text{NO}_2$  can bond to metals in coordination compounds in numerous ways,<sup>10</sup> the  $C_{2v}$  symmetry of the adsorbed  $\text{NO}_2$  surface complex identified in this study reduces the number of specific bonding configurations that need to be considered to two. The two isomers are nitro (I) and O,O'-nitrito (II) or chelating. A nitrate species (III) with  $C_{2v}$  symmetry must also be considered since the high coverages of oxygen atoms present on the surface at the time of  $\text{NO}_2$  adsorption present the possibility that an  $\text{NO}_3$  species could be formed. However, it would be expected from the vibrational spectra of coordination compounds containing  $\text{NO}_3$  that a dipole-active mode at approximately 1000  $\text{cm}^{-1}$  due to the MO- $\text{NO}_2$  stretch<sup>14</sup> would be observed if III were formed on the surface. Outka et al.<sup>13</sup> have proposed the existence of III with  $C_{2v}$  symmetry on Ag(110) and have assigned an HREELS energy loss at 1080  $\text{cm}^{-1}$  to the AgO- $\text{NO}_2$  stretch. At no coverage of oxygen atoms and  $\text{NO}_2$  is such a vibrational frequency observed in this work.

The vibrational frequencies of  $C_{2v}$   $\text{NO}_2$  adsorbed on oxygen atom saturated Pt(111) match those of  $\text{NO}_2$  nitro bonded on Ru(001) very well. Both are listed in Table I for comparison. The intensity of the bend relative to the symmetric stretch is also remarkably similar in the two cases. This implies that  $\text{NO}_2$  is bonded in the same configuration on both surfaces. To a large extent, then, the discussion put forth by Schwalke et al.<sup>2</sup> that compares the nitro and chelating bonding geometries can be used to argue that  $\text{NO}_2$  is also nitro-bonded on oxygen atom saturated Pt(111). Also, the vibrational frequency of the nitro  $\text{NO}_2$  symmetric stretch in  $\text{Pt}(\text{NO}_2)_4$ <sup>2-10</sup> given in Table I is only 75  $\text{cm}^{-1}$  higher than the frequency of  $C_{2v}$   $\text{NO}_2$  on Pt(111). However, the typical frequencies of the symmetric stretch for  $\text{NO}_2$  bonded as a chelate in transition-metal complexes are close too, having a range 1171-1225  $\text{cm}^{-1}$ .<sup>10,15</sup>

In view of the preceding discussion, it is obvious that an identification of the bonding geometry based only on the small frequency differences between the symmetric

(11) Ibach, H.; Mills, D. L. *Electron Energy Loss Spectroscopy and Surface Vibrations*; Academic: New York, 1982.

(12) Koel, B. E. In *Scanning Electron Microscopy/1985/IV*; SEM, AMF: O'Hare, IL, 1985; p 1421.

(13) Outka, D. A.; Madix, R. J.; Fisher, G. B.; Dimaggio, C. *Surf. Sci.* 1987, 179, 1.

(14) Addison, C. C.; Gatehouse, B. M. *J. Chem. Soc.* 1960, 613.

(15) Nakamoto, K. *Infrared and Raman Spectra of Inorganic and Coordination Compounds*, 4th ed.; John Wiley & Sons: New York, 1986.

(16) Arakawa, E. T.; Nielson, A. H. *J. Mol. Spectrosc.* 1958, 2, 413.

stretches of nitro and chelating  $\text{NO}_2$  ligands in transition-metal coordination compounds cannot be an unambiguous one. From the standpoint of steric hindrance and  $\text{NO}_2$  coverage, however, the nitro species is a strong assignment. I certainly takes up less room on the surface than II. The established chemical preference of Pt(111) to adsorb  $\text{NO}_2$  in a bridge-bonded geometry<sup>1</sup> suggests that an ensemble of Pt atoms large enough to adsorb II should instead adsorb bridge-bonded  $\text{NO}_2$ . The adsorption of II would also require the unreasonable "total site" occupancy of greater than 1 ML for the  $\text{NO}_2$  saturation coverage of 0.15 ML (effectively 0.3 ML considering the bidentate nature of II) coadsorbed with the oxygen atom saturation coverage of 0.75 ML.

The assignment of nitro-bonded  $\text{NO}_2$  is further supported by the intensity of the ONO bend relative to the intensity of the ONO symmetric stretch. The perpendicular displacement of nonbonded oxygen atoms in I during a bending vibration should contribute to a dynamic dipole that is quite large and therefore an energy loss that is more intense than that for II. Of course this argument needs a reference HREELS spectrum of chelating  $\text{NO}_2$  bonded to a surface to be convincing. Such a species has recently been identified by us on Au(111).<sup>3</sup> The intensity of the bending mode relative to the symmetric stretch is indeed noticeably less than the same modes of  $C_{2v}$   $\text{NO}_2$  adsorbed on oxygen-saturated Pt(111). Also, the symmetric stretching frequency for the chelating species is  $1180\text{ cm}^{-1}$ . This is in close agreement with the symmetric stretching frequency of  $\text{NO}_2$  coordinated as a chelate in transition-metal complexes.<sup>10,15</sup> Therefore, I and II have unique vibrational spectra that can be used to distinguish one from the other.

No evidence of other vibrational modes due to impact scattering was found in the off-specular HREELS spectra of  $\text{NO}_2$  adsorbed on the oxygen atom saturated Pt(111) surface. This implies that the  $\text{NO}_2$  asymmetric stretching frequency may be very close to the frequency of the symmetric stretch at  $1270\text{ cm}^{-1}$ . The possible near degeneracy of these two modes may be expected since the frequency difference between the two stretching modes of nitro-coordinated  $\text{NO}_2$  in transition-metal complexes is typically less than  $100\text{ cm}^{-1}$ .<sup>10,15</sup>

**Adsorption Kinetics.** An important result of this work is the finding that even at high oxygen atom precoverages  $\text{NO}_2$  is adsorbed with a high probability and with a reasonably strong chemical bond. The sticking coefficient of unity below 170 K that is insensitive to the coverage of both oxygen atoms and  $\text{NO}_2$  suggests the possibility that a metastable  $\text{NO}_3$  precursor species may play a role in the efficient uptake of  $\text{NO}_2$  on the oxygen-precovered surface. However, this species was not observed with HREELS. The fact that only a small saturation coverage of 0.15 ML of  $\text{NO}_2$  can be attained for the chemisorbed state on the oxygen atom precovered surface lends stoichiometric support to the determination that a stable  $\text{NO}_3$  is not formed on the surface.

The coverage of irreversibly adsorbed  $\text{NO}_2$  is determined by the oxygen atom coverage and decreases linearly as the oxygen coverage goes up. The total chemisorbed  $\text{NO}_2$  coverage might have the same dependence on oxygen atom coverage if it was not for the adsorption of  $\text{NO}_2$  in a nitro-bonded geometry. This bonding configuration keeps the  $\text{NO}_2$  uptake from going to zero on the oxygen atom saturated surface and contributes to the amount of reversibly adsorbed  $\text{NO}_2$  being essentially constant with oxygen atom coverage.

Even though the surface bond is weak at 11 kcal/mol, nitro-bonded  $\text{NO}_2$  is not incorporated into the multilayer.

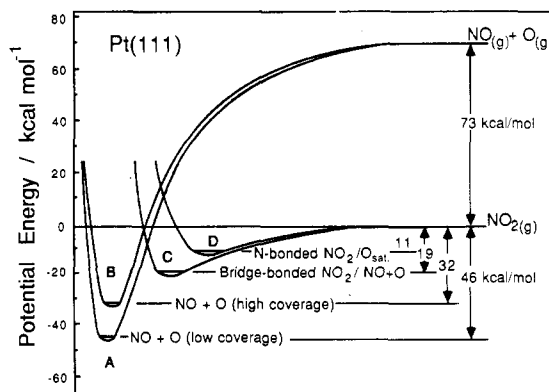


**Figure 9.** Schematic potential energy curves for the Pt(111)  $\mu$ -N,O-nitrito surface complex (bridge-bonded  $\text{NO}_2$ ), its decomposition products, and the Pt(111) nitro surface complex (nitro-bonded  $\text{NO}_2$ ) in the presence of oxygen atoms on Pt(111).

This follows a thermodynamic reasoning that has been applied previously to explain the behavior of  $\text{NO}_2$  adsorbed on clean Pt(111).<sup>1</sup> Nitro-bonded  $\text{NO}_2$  is a true chemisorbed species with a well-defined bonding geometry.

**Desorption from the Multilayer.** The existence of a metastable, short-lived  $\text{NO}_3$  species formed from the decomposition of  $\text{N}_2\text{O}_4$  to  $\text{NO}_2$  on the oxygen-saturated surface when heated during TPD could explain the  $\text{NO}_2$  first-order desorption peak at 155 K from a state that has a vibrational spectrum clearly that of  $\text{N}_2\text{O}_4$ . The amount of  $\text{N}_2\text{O}_4$  associated with this state is about 0.25 ML. More importantly, this means that 0.5 ML of  $\text{NO}_2$  would be available from this state. This amount of  $\text{NO}_2$  approaches the one-to-one correspondence with the oxygen atom coverage of 0.75 ML that might be expected if the formation of an  $\text{NO}_3$  transient was favorable. This is a reasonable possibility in view of  $\text{NO}_2$  desorption from the  $\text{N}_2\text{O}_4$  multilayer present on Pt(111) saturated with bridge-bonded  $\text{NO}_2$ . For this case, desorption from the initial  $\text{N}_2\text{O}_4$  monolayer takes place with zero-order kinetics since no oxygen atoms are available and metastable  $\text{NO}_3$  cannot be formed. The presence of two zero-order desorption states shown in Figure 5 must be the result of a slight energetic difference between  $\text{NO}_2$  desorption from a  $\text{N}_2\text{O}_4$  layer that is on top of another  $\text{N}_2\text{O}_4$  layer and  $\text{NO}_2$  desorption from a  $\text{N}_2\text{O}_4$  layer that is on top of a bridge-bonded  $\text{NO}_2$  layer.

**Adsorption Geometry Requirements for Dissociation.** In Figure 9, schematic potential energy diagrams for each of the three states in which  $\text{NO}_2$  is known to exist on Pt(111) are placed on the same reaction coordinate with zero energy being referenced to gas-phase  $\text{NO}_2$ . Although qualitative in shape they are quantitative in depth, using data from this work and ref 1. For the purpose of this discussion, the curves' crossing points adequately illustrate the influence of kinetic barriers on the observed behavior of  $\text{NO}_2$  on clean and on oxygen-covered Pt(111). The curves are used to discuss the dependence that  $\text{NO}_2$  dissociation has on its adsorption geometry. As such, the role of bridge-bonded  $\text{NO}_2$  as the necessary precursor to dissociation on the Pt(111) surface is emphasized.

Previous work<sup>1</sup> has shown that at low coverages molecular adsorption of  $\text{NO}_2$  at 100 K on clean Pt(111) is followed by complete dissociation at 170 K to yield oxygen atoms and NO. The potential energy curve for these products has a well depth of 46 kcal/mol and is represented by curve A in Figure 9. The well-depth for oxygen atoms and NO is diminished continuously with increasing NO and oxygen atom coverage until  $\theta_{\text{O}+\text{NO}} = 0.5$  ML. It is at this point that a constant well depth of 32 kcal/mol is reached (curve B) and  $\text{NO}_2$  desorption becomes com-

petitive with its decomposition. The potential energy curve for NO<sub>2</sub> under these conditions is represented by curve C and is associated with bridge-bonded NO<sub>2</sub>. It has a depth of 19 kcal/mol that is constant over a large range of NO<sub>2</sub>, NO, and oxygen atom coverages. The crossing point of B and C, elevated with respect to the crossing point of A and C, qualitatively depicts that when the potential energy curve of the dissociation products NO and oxygen atoms is lifted to 32 kcal/mol, a kinetic barrier is formed that is of sufficient height to allow some reversible adsorption of NO<sub>2</sub> to take place. In further agreement with this representation is the fact that at no coverage up to saturation in the chemisorbed NO<sub>2</sub> monolayer does decomposition cease being competitive with desorption. In addition, the NO<sub>2</sub> that desorbs does so exclusively with first-order kinetics, indicating that the height of the barrier for NO and oxygen atoms to recombine and form NO<sub>2</sub> is higher than the barrier to NO desorption.<sup>1,8</sup>

The existence of NO<sub>2</sub> in numerous weakly bound adsorption geometries has been postulated<sup>1</sup> to explain the high sticking coefficient of NO<sub>2</sub> on Pt(111).<sup>1,6</sup> The results reported in this paper make it clear that one of the precursors that could play an important role in adsorption to form bridge-bonded NO<sub>2</sub> may be nitro-bonded NO<sub>2</sub>. The kinetic barrier between bridge-bonded NO<sub>2</sub> and nitro-bonded NO<sub>2</sub> is too low on clean Pt(111) for nitro-bonded NO<sub>2</sub> to be stable on the HREELS time scale. However, in a manner consistent with our HREELS observations, the diagrams in Figure 9 show how nitro-bonded NO<sub>2</sub> (curve D) can be stabilized if the possibility for bridge-bonded adsorption (curve C) is removed. By simple steric inhibition, coadsorbed oxygen atoms not only can reduce the amount of NO<sub>2</sub> adsorbed but at a saturation coverage of  $\theta_{\text{O}} = 0.75$  ML can also remove any Pt ensembles large enough to allow a bridge-bonded configuration to be achieved. To overcome this, the displacement of at least one oxygen atom on the surface by an oxygen atom from bridge-bonded NO<sub>2</sub> would be required. This would be thermodynamically unreasonable. Therefore, with the bridge-bonded adsorption geometry no longer available, curve C is effectively removed from the diagram in Figure

9, and decomposition of nitro-bonded NO<sub>2</sub> is eliminated by the large barrier represented by the crossing point of curves B and D. Thus, NO<sub>2</sub> coadsorbed with 0.75 ML of oxygen atoms on Pt(111) is restricted to a nitro-bonding geometry, and simultaneous contact between the Pt surface, the oxygen atom, and the nitrogen atom cannot be achieved. As a result, NO<sub>2</sub> cannot dissociate to oxygen atoms and NO. Recently, we have used HREELS and TPD to prove that a true barrier exists for the reverse case by showing that NO coadsorbed with high coverages of oxygen atoms on Pt(111) does not form NO<sub>2</sub>.<sup>8</sup>

### Summary

The coadsorption of NO<sub>2</sub> and oxygen atoms on Pt(111) has been studied. Changes in the NO<sub>2</sub> coverage, adsorption energy, and the adsorption geometry have been observed as a function of oxygen atom precoverage. When  $\theta_{\text{O}} \geq 0.25$  ML, a new chemisorption state for NO<sub>2</sub> is stabilized. NO<sub>2</sub> is bonded directly to a platinum atom via the nitrogen atom in a nitro configuration with C<sub>2v</sub> symmetry. This is the exclusive bonding geometry for NO<sub>2</sub> when it is coadsorbed with 0.75 ML of oxygen atoms on Pt(111). TPD has been used to determine that this chemisorbed state has a heat of adsorption of 11 kcal/mol and can be populated to a saturation coverage of 0.15 ML of NO<sub>2</sub>. NO<sub>2</sub> chemisorption takes place with an initial sticking coefficient of unity at temperatures below 170 K and is completely reversible on the oxygen atom saturated surface. There is no coverage at which a stable NO<sub>3</sub> species is formed from the coadsorption of NO<sub>2</sub> and oxygen atoms on Pt(111) at 100 K. However, a short-lived NO<sub>3</sub> intermediate is proposed to explain the strong precursor adsorption kinetics and a first-order desorption feature in TPD of the first physisorbed N<sub>2</sub>O<sub>4</sub> layer.

**Acknowledgment.** Financial support for this work from the National Science Foundation through a grant given to Sievers Research Inc. as a part of the SBIR program contract No. IFI-8521288 and the National Acid Precipitation Assessment Program is gratefully acknowledged.

**Registry No.** NO<sub>2</sub>, 10102-44-0; O, 17778-80-2; Pt, 7440-06-4.

## Coadsorption of Hydrocarbon Fragments with CO on Ni(100) and Ru(001)<sup>†,‡</sup>

S. Akhter, M. A. Henderson, G. E. Mitchell, and J. M. White\*

Department of Chemistry, University of Texas, Austin, Texas 78712

Received July 17, 1987. In Final Form: September 9, 1987

The coadsorption of CO with C<sub>2</sub> hydrocarbon fragments was studied on Ni(100) and Ru(001). The hydrocarbon intermediates included vinyl, ethylidyne, acetylinic/vinylidene, and acetylide species. These fragments exhibited greater thermal stability in the presence of high coverages of coadsorbed CO. The stabilization is mainly attributed to a site-blocking effect of CO. The implications of this effect for Fisher-Tropsch synthesis are considered in detail.

### Introduction

Under Fisher-Tropsch (F-T) synthesis conditions, various known and postulated hydrocarbon fragments,<sup>1-4</sup>

viz., C, CH<sub>x</sub>, and C<sub>n</sub>H<sub>m</sub>, coexist with a large amount of coadsorbed CO, which nearly saturates the metal surface.<sup>5</sup> Any interaction between CO and the hydrocarbon fragments is expected to influence the mechanistic and kinetic

<sup>†</sup> Presented at the symposium entitled "Molecular Processes at Solid Surfaces: Spectroscopy of Intermediates and Adsorbate Interactions", 193rd National Meeting of the American Chemical Society, Denver, CO, April 6-8, 1987.

<sup>‡</sup> Supported in part by the National Science Foundation (CHE 8505413), the Exxon Education Foundation, and the Robert A. Welch Foundation.

(1) Bell, A. T. *Catal. Rev. Sci. Eng.* 1981, 23, 203.  
 (2) Rofer-De Poorter, C. K. *Chem. Rev.* 1981, 81, 447.  
 (3) Ponc, V. *Catal. Rev. Sci. Eng.* 1978, 18, 151.  
 (4) Ponc, V. In *Catalysis*; Bond, G. C., Web, G., Eds.; Specialist Periodical Reports; The Chemical Society: London, 1982; Vol. 5, p 48.  
 (5) Ekerdt, J. G.; Bell, A. T. *J. Catal.* 1979, 58, 170.